IEEE Photonics Journal
An IEEE Photonics Society Publication

Open Access

A Dual-Wavelength Rational Harmonic Mode-Locked Fiber Ring Laser With Different Repetition Frequencies

Volume 7, Number 2, April 2015

Yuejiao Zi
Yang Jiang, Member, IEEE
Chuang Ma
Guangfu Bai
Zhenrong Jia
Tingwei Wu
Fengqin Huang

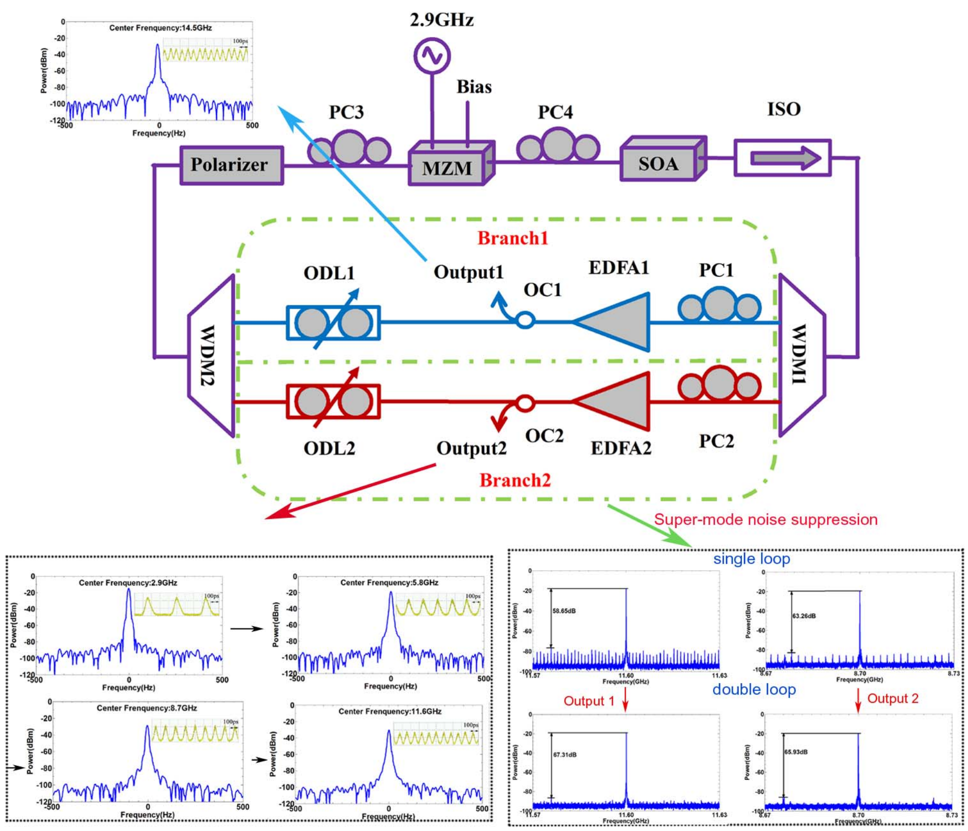

DOI: 10.1109/JPHOT.2015.2417167
1943-0655 © 2015 IEEE

A Dual-Wavelength Rational Harmonic Mode-Locked Fiber Ring Laser With Different Repetition Frequencies

Yuejiao Zi, Yang Jiang, *Member, IEEE*, Chuang Ma, Guangfu Bai, Zhenrong Jia, Tingwei Wu, and Fengqin Huang

Department of Physics, School of Science, Guizhou University, Guiyang 550025, China

DOI: 10.1109/JPHOT.2015.2417167

Manuscript received February 3, 2015; revised March 15, 2015; accepted March 22, 2015. Date of publication March 26, 2015; date of current version April 10, 2015. This work was supported in part by the National Natural Science Foundation of China under Grant 61061004 and Grant 61465002, by the Program for New Century Excellent Talents in University of the Ministry of Education of China under Grant NCET-10-0099, and by the college innovation talent team of Guizhou province (2014) 32. Corresponding author: Y. Jiang (e-mail: jiangyang415@hotmail.com).

Abstract: A dual-wavelength rational harmonic mode-locked fiber ring laser with different repetition frequencies is theoretically analyzed and experimentally demonstrated. In this scheme, two wavelength channels are inserted into the laser loop to form two resonant cavities. By tuning the length of each channel, required rational harmonic mode-locking conditions can be achieved, and dual-frequency mode-locked signals are simultaneously generated at different wavelengths. In addition, the supermode suppression ratio is further improved due to the mode competition caused by this dual-cavity configuration. In the experimental demonstration, when the fourth-order (or fifth-order) harmonic mode-locked signal is generated in Cavity 1, the first-, second-, and third-order (or fourth-order) harmonic mode-locked signals, respectively, can be generated in Cavity 2 by tuning its length. The measured radio frequency spectra and waveforms show that the signals have high quality. Compared with a conventional rational harmonic mode-locked laser (RHMLL), more than 10 dB supermode suppression ratio improvement is obtained. Since this system can flexibly implement multiwavelength and multifrequency signal generation without adding much cost, it may have wide applications in optical communication system, photonic microwave signal generation, and optical waveform synthesizers.

Index Terms: Mode locking, rational harmonic mode-locking (RHML), fiber laser, supermode suppression, semiconductor optical amplifier, dual-wavelength, dual-frequency, signal generation.

1. Introduction

High-repetition-frequency optical pulses and clock signals have wide applications in modern optical communication systems, such as the time division multiplexing (TDM) system [1], [2] and all-optical signal processing [3]. For generating such signals, the mode-locked fiber ring laser (ML-FRL) is an effective way and can be carried out by using passively mode-locking (PML) or actively mode-locking (AML) technique. In the passively mode-locked laser, nonlinear optical elements are exploited to achieve phase locking among fundamental cavity modes, for example, the saturable absorber (SA) [4], [5], the nonlinear polarization rotation (NPR) [6], the nonlinear amplifying loop mirror (NALM) [7], etc. However, the PML technique has a serious

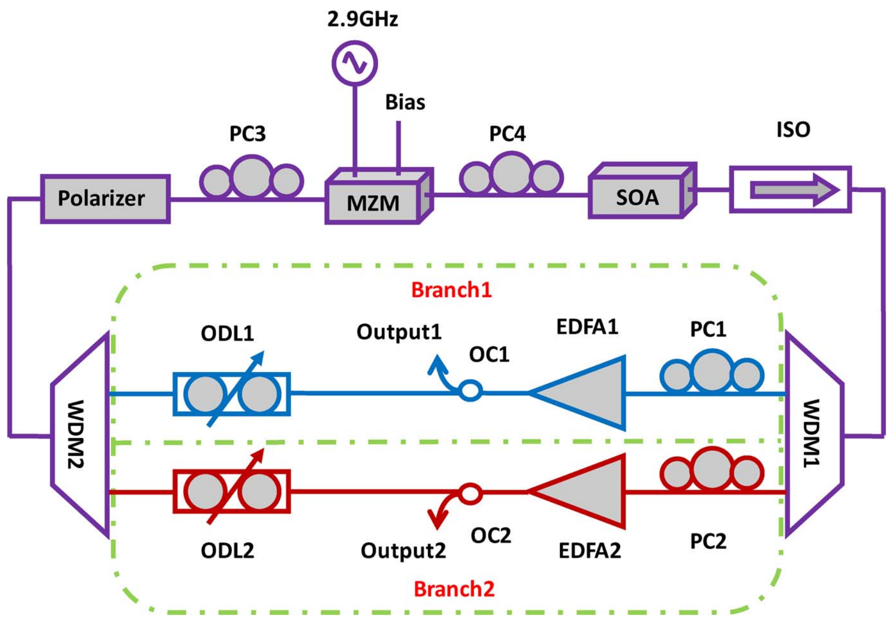

Fig. 1. Configuration of the proposed dual-wavelength dual-repetition-frequency RHMLL.

drawback that the output repetition frequency from a passively mode-locked laser is difficult to reach GHz scale due to the relatively long laser cavity, which limits its applications. For the actively mode-locked laser, a modulator is inserted into the laser cavity to force parts of longitudinal modes to be coupled and the locked frequency f_p equals to the driven frequency f_m. However, this approach suffers operation bandwidth restriction of the modulator and it is impossible to generate optical pulses with a repetition frequency higher than f_m. Fortunately, this shackle can be broken by RHML technique, which has been used for high-repetition-frequency optical pulse generation and photonic microwave signal multiplication. In this method, by properly arranging the relationship between cavity mode spacing and modulation frequency, the axial modes apart of a multiple of f_m can be coupled and the mode-locked output has frequency of several times of f_m. In general, although some remaining uncoupled axial modes may cause super-mode noise and make the signal with unequal amplitude, various solutions have been suggested to deal with this problem, such as dithering the erbium fiber [8], installing a semiconductor optical amplifier (SOA) [9], [10], and incorporating an etalon [11] as a filter. It should be noticed that RHMLLs can break the modulator operation bandwidth limitation, but only one signal with a certain frequency and wavelength is generated, which has low spectrum efficiency and the flexibility loss since the gain medium and other optical components are still broadband devices.

In this paper, a dual-wavelength RHMLL with two repetition frequencies is proposed and demonstrated. This RHMLL has two optical cavities at different operation wavelengths. It can independently implement rational harmonic mode-locking at each wavelength by adjusting the corresponding cavity length. A SOA is employed as gain medium for two sets of cavity modes and can stabilize the outputs. As far as we know, this is the first time that a dual-wavelength RHMLL with different repetition frequencies has been reported. The experimental results show this RHMLL has flexible outputs with high quality. In addition, the super-mode suppression ratio is better than that of conventional single cavity RHMLLs.

2. Principle

The configuration of the proposed scheme is shown in Fig. 1. This system is similar to a conventional RHMLL but there are two cavities operating at different wavelengths. In the main loop, a polarizer before a Mach–Zehnder modulator (MZM) forces two light fields in the same polarization state, and the MZM is driven by a RF signal at frequency of f_m. An SOA is used as gain medium and simultaneously suppresses the super-mode noise. An isolator (ISO) is inserted into the main loop to ensure the light propagating in clockwise direction. Two wavelength division multiplexers (WDM) play roles of bandpass filters and construct two optical branches. In each branch, an erbium-doped fiber amplifier (EDFA) is used to compensate the insertion loss of optical components and a tunable optical delay line (ODL) is able to adjust the path length for desired cavity length. A polarization controller (PC) aligns the polarization state of the light field and an optical coupler (OC) is employed to extract the generated signal.

Obviously, the configuration is equivalent to a conventional mode-locked laser if either branch is disconnected. In this case, when the laser reaches threshold condition, the excitation light field is generated with a group of cavity modes due to the characteristic of the ring cavity. The frequency spacing between two adjacent cavity modes is $f_c = c/(n_{eff} L)$, where c is the speed of light in vacuum, n_{eff} is the efficient index in the cavity, and L is the length of the ring cavity. The MZM with driven frequency f_m is used to modulate these cavity modes. According to the relationship between f_c and f_m, AML or RHML operation can be achieved [12]–[16].

In the case of AML, f_m is n times of f_c (n is an integer). $a_q^{(k)}$ is the amplitude of the q^{th} mode when light passes the k^{th} circle (q and k are integers). Assuming that the modulation depth is $M[1 - cos(2\pi f_m t)]$, the equation for $a_q^{(k)}$ can be given by [15]

$$a_q^{(k+1)} = a_q^{(k)} + g\left[1 - \frac{(2\pi q f_c)^2}{\Omega_g^2}\right] a_q^{(k)} - l a_q^{(k)} + \frac{M}{2}\left(a_{q+n}^{(k)} - 2a_q^{(k)} + a_{q-n}^{(k)}\right) \tag{1}$$

where g is the gain constant, l is the loss constant, and Ω_g is the gain bandwidth. In (1), the q^{th} mode is related to $(q+n)^{\text{th}}$ and $(q-n)^{\text{th}}$ modes in participation of the modulator. When oscillation bandwidth is sufficiently broad, steady-state solution is obtained as

$$a(t) = \frac{\sqrt{2}\pi}{\tau} A e^{-t^2/2\tau^2} \tag{2}$$

where A is a constant, and $\tau = (2g/M)^{1/4}(1/2\pi f_m \Omega_g)^{1/2}$. Equation (2) shows that the mode-locking operation makes the fiber laser output pulse trains. When q is replaced by $q+1, q+2, \ldots, q+n-1$ in (1), the equation keeps the same form. Hence, there exist n sets of modes in the cavity. In time domain, n pulses circulate in the cavity with length of L at the same time. Therefore, repetition frequency is rewritten as

$$f_p = n f_c = f_m. \tag{3}$$

For the RHML case, f_m is $(n + (1/p))$ times f_c, where p is an integer. In this situation, (1) is written as

$$a_q^{(k+1)} = a_q^{(k)} + g\left[1 - \frac{(2\pi q f_c)^2}{\Omega_g^2}\right] a_q^{(k)} - l a_q^{(k)} + \frac{M}{2}\left(a_{q+n+\frac{1}{p}}^{(k)} - 2a_q^{(k)} + a_{q-n-\frac{1}{p}}^{(k)}\right). \tag{4}$$

Because $(q \pm n \pm (1/p))^{\text{th}}$ mode cannot exist in the L-length cavity, an equivalent cavity with length of pL is taken into account. Equation (4) is rewritten as

$$a_{q'}^{(k+1)} = a_{q'}^{(k)} + g\left[1 - \frac{\left(2\pi \frac{q}{p} f_c\right)^2}{\Omega_g^2}\right] a_{q'}^{(k)} - l a_{q'}^{(k)} + \frac{M}{2}\left(a_{q'+n+\frac{1}{p}}^{(k)} - 2a_{q'}^{(k)} + a_{q'-n-\frac{1}{p}}^{(k)}\right) \tag{5}$$

where $q' = np$. In (5), q'^{th} mode can be coupled to $(q' + np + 1)^{\text{th}}$ and $(q' - np - 1)^{\text{th}}$ modes. Compared with (1), there are $(np + 1)$ sets of modes in the cavity, which means that $(np + 1)$

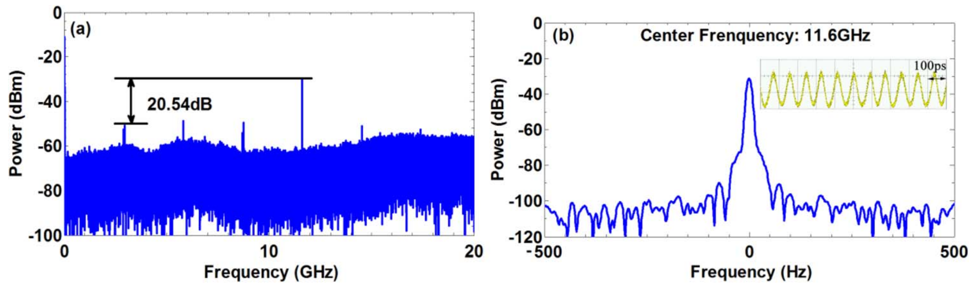

Fig. 2. RF spectra and waveform of the signal from Cavity 1 with repetition frequency of $4f_m$, where $f_m = 2.9$ GHz. (a) RF spectrum with span of 20 GHz. (b) Zoom-in RF spectrum with span of 1 kHz. (Inset) Corresponding waveform.

pulses simultaneously operate in the L-length cavity. Therefore, the repetition frequency is obtained as

$$f_p = (np + 1)f_c = pf_m. \tag{6}$$

Equation (6) shows that the frequency multiplication is achieved.

Let us consider the two-cavity situation shown in Fig. 1. Here, two branches, i.e., Branch 1 and Branch 2, are associated with the main loop to form two cavities, called Cavity 1 and Cavity 2. When the two cavities simultaneously satisfy the RHML conditions, two signals with different repetition frequencies, $p_1 f_m$ and $p_2 f_m$, can be obtained, where p_1 and p_2 are integers. In the proposed system, a SOA is placed in the main loop and nonlinear modulation effect may be introduced, since carriers in the SOA are shared by two sets of cavity modes. However, according to (6), if the p_1 is different from p_2, the fundamental cavity frequency f_{c1} in Cavity 1 must not be equal to f_{c2} in Cavity 2, which means that these two sets of modes are hard to be coupled with each other. Even so, the mode competition effect may lead to further super-mode suppression. Therefore, this dual-cavity architecture has potential to obtain a higher super-mode suppression ratio than that of conventional configurations.

3. Experimental Results and Discussion

Based upon the setup shown in Fig. 1, an experiment is performed. A polarizer and PC3 are used to ensure the two optical fields with same modulation efficiency. The MZM has bandwidth of 20 GHz and is driven by a RF signal at frequency of 2.9 GHz. The followed SOA (Thorlabs Quantum Electronics, SOA-17415-11450.29.C01) with injection current of 390 mA provides optical gain for both signals. In order to form dual-wavelength channels, a pair of WDMs with bandwidth of 0.8 nm on each channel is employed and the ODLs between them can adjust the lengths of two cavities for required RHML conditions. An EDFA is placed in each branch for compensating the cavity loss and making two optical fields with equal power. From the two 20% ports of the OCs, the signals are extracted and measured by an optical spectrum analyzer (OSA, Yokogawa AQ6370C), an electrical spectrum analyzer (ESA, Agilent N9010A EXA), and an oscilloscope (Agilent 86100D Infiniium DCA-X).

3.1. The Dual-Wavelength RHMLL With Different Repetition Frequencies

First, we fix an even order mode-locking in Cavity 1 and tune the other cavity length, where the center wavelengths of 1550.92 nm for Cavity 1 and 1549.32 nm for Cavity 2 are selected. In this case, the modulation frequency f_m is set to be 2.9 GHz and a 4th-order harmonic signal in Cavity 1 is obtained by properly adjusting ODL1 and PC1. The corresponding measurement is shown in Fig. 2. Fig. 2(a) is the RF spectrum, in which a strong fourth-order harmonic is observed and the power is 20.54 dB higher than that of the fundamental modulation component. Meanwhile, the 2nd-order and 3rd-order components are well suppressed. The zoom-in RF spectrum is shown in Fig. 2(b). It shows that the signal has high spectral purity, low noise, as

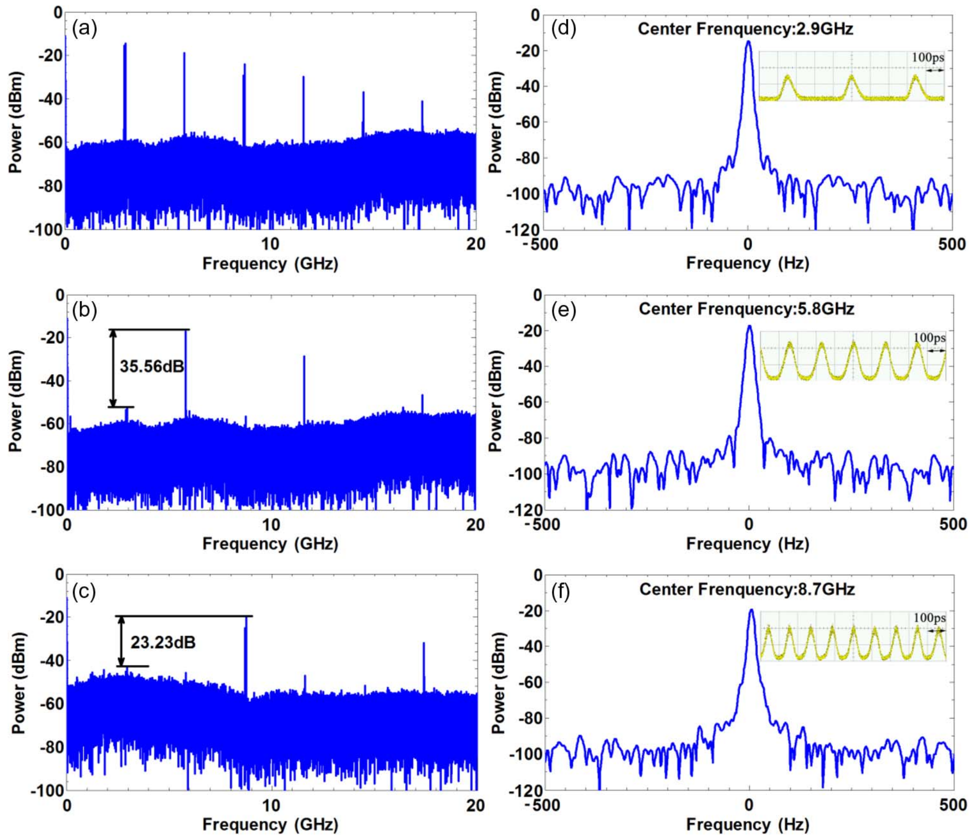

Fig. 3. RF spectra and waveforms of the signals from Cavity 2, where $f_m = 2.9$ GHz. (a)–(c) RF spectra of the signals with repetition frequencies of f_m, $2f_m$, and $3f_m$, respectively. (d)–(f) Corresponding zoom-in RF spectra. (Insets) Corresponding waveforms.

well as a clean and stable waveform. When Cavity 1 keeps unchanged, different harmonic mode-locked signals with repetition frequencies of f_m, $2f_m$ and $3f_m$ can be achieved by gradually tuning ODL2 in Cavity 2. Fig. 3(a)–(f) gives the corresponding RF spectra and waveforms. In Fig. 3(a) and (d), the component at f_m is locked and many high order harmonics appear since the corresponding waveform is a narrow optical pulse train. By varying ODL2, the situations of RHML occur and harmonics can be locked at $2f_m$ and $3f_m$, respectively. In Fig. 3(b), the frequency component of 5.8 GHz ($2f_m$) is the dominate one with the modulation frequency suppression ratio of 35.56 dB. The detailed RF spectrum and waveform in Fig. 3(e) also show the signal has high quality. The results of the 3rd-order rational harmonic mode-locking from Cavity 2 are shown in Fig. 3(c) and (f). As shown in the figures, a strong and clean signal with repetition rate of 8.7 GHz is generated.

To further demonstrate the flexibility, another set of experimental measurements based on the same setup is performed. Here the operation wavelengths are selected at 1550.92 nm for Branch 1 and 1552.52 nm for Branch 2. Fig. 4 shows the measurements of the 5th-order, which is an odd order, rational harmonic mode-locked signal in Cavity 1 while Fig. 5 gives the situations of the signals with repetition frequencies of f_m, $2f_m$, $3f_m$, and $4f_m$ in Cavity 2, respectively. Obviously, these figures display results very similar to the first experiment, which indicate that the proposed system has the ability to generate two signals with required harmonic frequencies in each cavity at the same time.

Just like conventional RHMLLs, the unequal amplitudes on mode-locked outputs can be observed in this scheme, especially when higher order rational harmonic mode-locking is performed. This phenomenon in this dual-cavity configuration has no visible difference compared

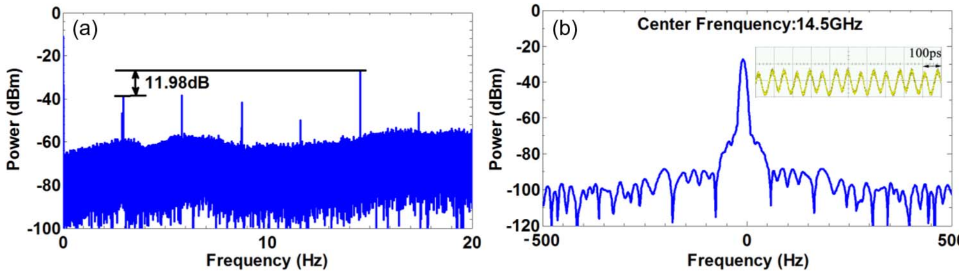

Fig. 4. RF spectra and waveform of the signal from Cavity 1 with repetition frequency of $5f_m$, where $f_m = 2.9$ GHz. (a) RF spectrum with span of 20 GHz. (b) Zoom-in RF spectrum with span of 1 kHz. (Inset) Corresponding waveform.

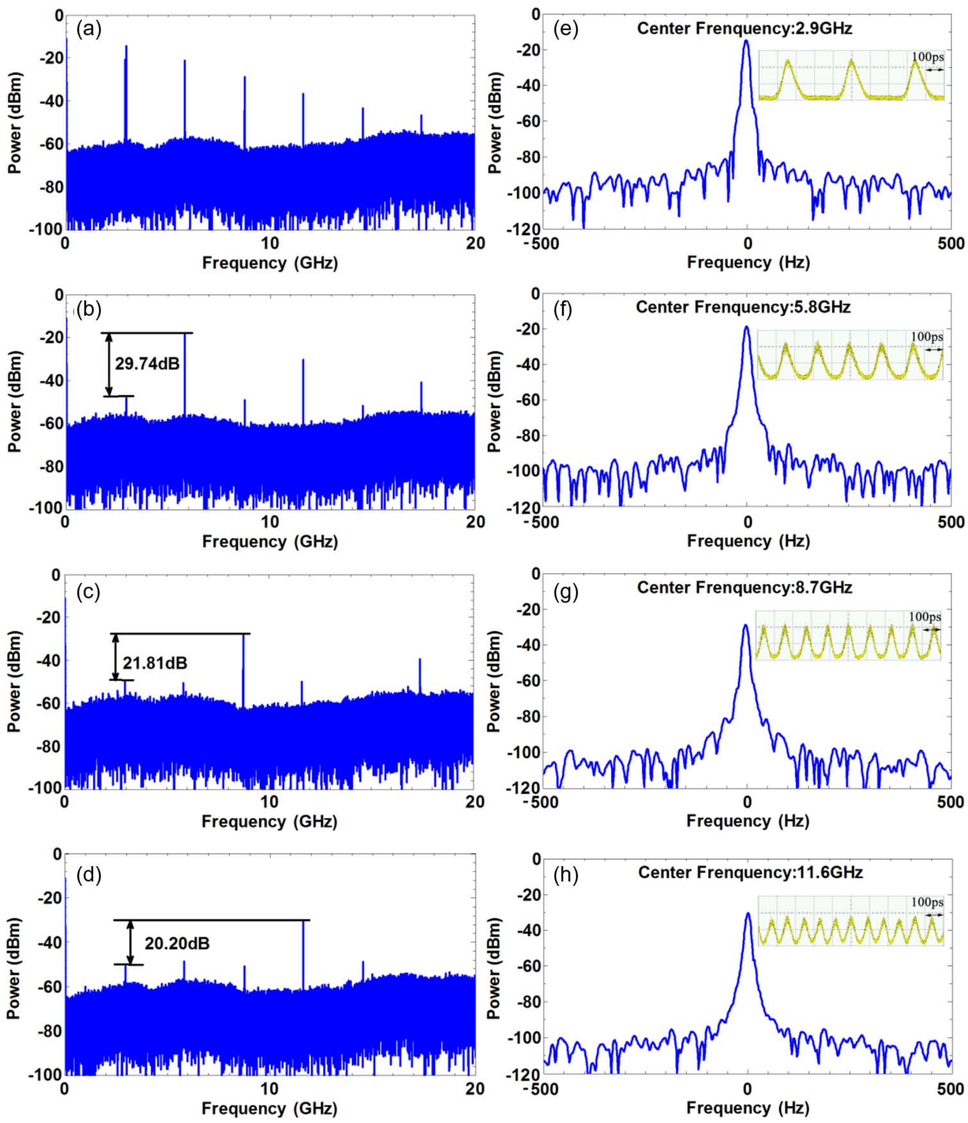

Fig. 5. RF spectra and waveforms of the signals from Cavity 2, where $f_m = 2.9$ GHz. (a)–(d) RF spectra of the signals with repetition frequencies of f_m, $2f_m$, $3f_m$, and $4f_m$, respectively. (e)–(h) Corresponding zoom-in RF spectra. (Insets) Corresponding waveforms.

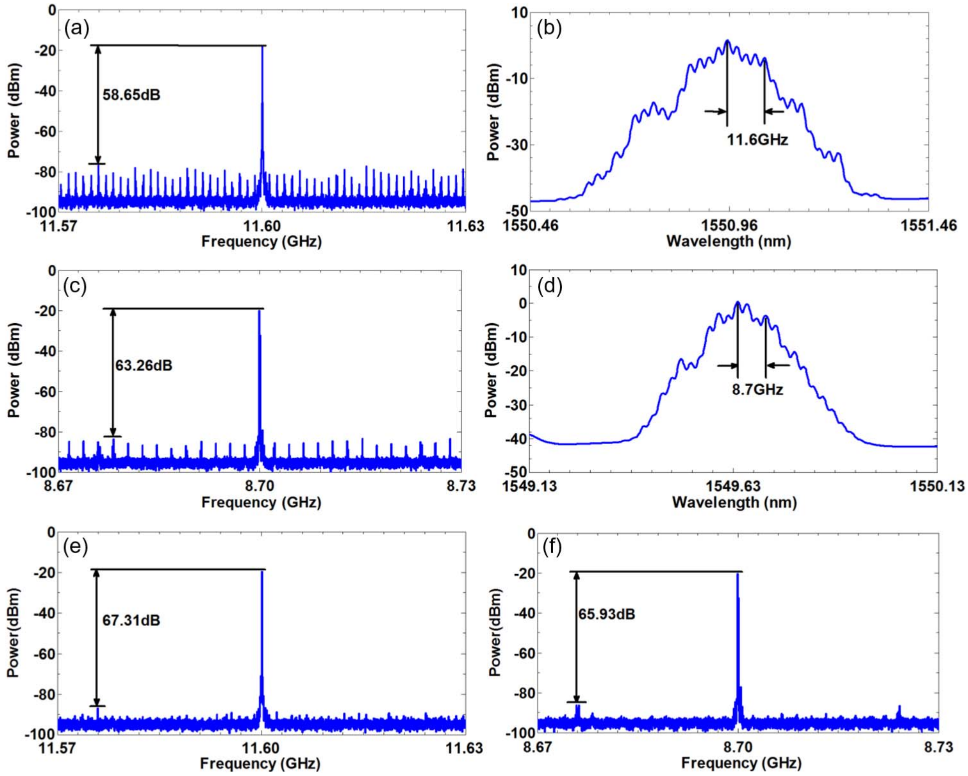

Fig. 6. Comparison of super-mode suppression effect, where $f_m = 2.9$ GHz. (a) RF spectrum and (b) corresponding optical spectrum of the fourth-order mode-locked signal from Cavity 1, when Cavity 2 is disconnected. (c) RF spectrum and (d) corresponding optical spectrum of the third-order mode-locked signal from Cavity 2, when Cavity 1 is disconnected. (e) and (f) Corresponding RF spectra of the signals generated by the dual-cavity RHMLL.

with the case of single cavity. Reasons for pulse amplitude imbalance in RHMLLs come from two aspects [17]–[20], which are super-mode noise and mismatched low-order harmonic components. This problem may be solved by using nonlinear modulation [19] or introducing an assistant filtering method [20] in the cavities.

According to the demonstration above, different mode-locked signals are simultaneously obtained in two cavities and the order of locked harmonics can be tuned by changing each cavity length. A pair of WDMs acts as the filters in two cavities, and therefore, the operation center wavelengths can be easily switched by selecting different channels of the WDMs. All results indicate that the scheme is a dual-repetition-frequency dual-wavelength RHMLL with higher spectrum efficiency and lower cost.

3.2. Super-Mode Suppression by the Dual-Cavity Configuration

As demonstration in 3.1, the proposed RHMLL contains two resonant cavities, in which there is a SOA shared by two mode-locked signals. In order to know how the two signals interact with each other, the case of fourth-order RHML in Cavity 1 and third-order RHML in Cavity 2 is chosen for detailed description. Firstly, the RF spectrum output from a single loop configuration is observed by breaking Cavity 2 or Cavity 1, respectively. When the RBW and VBW are set to be 18 kHz and 330 Hz, as shown in Fig. 6(a) and (c), the super-modes can be clearly seen from the RF spectra. One can read that the mode spacing is 1.098 MHz for Cavity 1 and 2.183 MHz for Cavity 2 and that the super-mode suppression ratios are 58.65 dB and 63.26 dB. From the corresponding optical spectra shown in Fig. 6(b) and (d), the mode-locked frequencies of 11.6 GHz and 8.7 GHz can also be observed and the operation wavelengths in two cavities are 1549.63 nm and 1550.96 nm, respectively. Then, when both cavities are connected, two rational harmonic mode-locked outputs can be simultaneously generated, and their waveforms have no visible change. In this case, the RF spectra are measured again, which are given by Fig. 6(e) and (f). When Fig. 6(e) is compared with Fig. 6(a), the power level and center frequency keep unchanged but the super-modes are dramatically suppressed. Even if the residual strongest super-mode is measured, the super-mode suppression ratio is improved to be 67.31 dB and the suppression ratio improvement for other super-modes is more than 10 dB. Similar results can also be found by a comparison between Fig. 6(c) and (f) when the signal from Cavity 2 is monitored in the same way.

Further explanations are tried to be given for understanding the super-mode suppression. In our experiment, the mode-locked signals in two cavities have optical power about −8 dBm, which is low but can slightly cause cross nonlinear modulation effects in the SOA to lead to mode competition. Since the interaction is weak and the locked modes are saturated, the carrier density fluctuation in the SOA does not affect the power of generated signal. However, the super-modes can be further suppressed by mode competition and only the common modes may appear. From another angle of view, as reported in [8], the two mode-locked signals propagate in the cavities, which cause a periodic carrier density fluctuation. This behavior can weakly dither two cavity lengths periodically and consequently suppress super-modes. In a word, a multi-cavity configuration is benefit for super-mode suppression, which has been widely confirmed and adopted in many oscillation systems, such as single-longitudinal-mode fiber lasers [21], [22], optoelectronic oscillators [23], [24]. This is an additional advantage for our proposed scheme.

From the results above, the system can realize simultaneous multi-wavelength mode-locking with different frequencies and better super-mode suppression. Although the results show no visible waveform change compared with conventional RHMLLs, the further suppressed super-mode noise may optimize the uneven amplitude to some extent. In our experiment, only dual-signal generation is performed, but it has potential to generate more optical signals with different frequencies by adding more channels with proper lengths. Those cavities may also lead to further super-mode suppression in addition to the conventional RHMLLs.

4. Conclusion

In conclusion, a novel dual-wavelength dual-frequency RHMLL is proposed and demonstrated. This system contains two resonant cavities with different operation wavelengths and cavity lengths, and it is able to generate dual-wavelength optical pulse trains with tunable repetition frequencies. The operation principle and super-mode suppression mechanism have been discussed. In the experimental demonstration, two cases of experimental measurements are preformed. One is the fourth-order harmonic mode-locked signal generated in Cavity 1 and the 1st-, second- and third-order harmonic mode-locked signals respectively generated in Cavity 2 by fine tuning its cavity length. The other experiment achieves one signal in Cavity 1 with frequency of 14.5 GHz (the 5th-order harmonic mode-locking) and the signals in Cavity 2 with repetition frequencies of 2.9 GHz, 5.8 GHz, 8.7 GHz, and 11.6 GHz, respectively. The center wavelengths of two signals can be switched by choosing different WDM channels. In addition, a higher super-modes suppression ratio is obtained because of the mode competition effect between two cavities. It is a cost-effective way and a functional system, which can be applied to flexible photonic microwave signal generation, optical communication system and optical waveform synthesizer.

References

[1] T. Kurosu, K. Tanizawa, and S. Namiki, “In-band clock distribution using signal phase for channel identifiable clock recovery in optical time-division multiplexing,” *Electron. Lett.*, vol 48, no. 14, pp. 863–864, Jul. 2012.

[2] Q. Nguyen-The, M. Matsuura, and N. Kishi, “WDM-to-OTDM conversion using supercontinuum generation in a highly nonlinear fiber,” *IEEE Photon. Technol. Lett.*, vol 26, no. 18, pp. 1882–1885, Sep. 2014.

[3] W. Wang *et al.*, “Tunable microwave frequency multiplication by injection locking of DFB laser with a weakly phase modulated signal,” *IEEE Photon. J.*, vol. 6, no. 2, Apr. 2014, Art. ID. 5500308.

[4] H. Zhang, D. Y. Tang, X. Wu, and L. M. Zhao, “Multi-wavelength dissipative soliton operation of an erbium-doped fiber laser,” *Opt. Exp.*, vol. 17, no. 15, pp. 12 692–12 697, Jul. 2009.

[5] M. Liu *et al.*, "Dual-wavelength harmonically mode-locked fiber laser with topological insulator saturable absorber," *IEEE Photon. Technol. Lett.*, vol. 26, no. 10, pp. 983–986, May 2014.

[6] Z. C. Luo *et al.*, "Tunable multiwavelength passively mode-locked fiber ring laser using intracavity birefringence-induced comb filter," *IEEE Photon. J.*, vol. 2, no. 4, pp. 571–577, Aug. 2010.

[7] L. Yun, X. M. Liu, and D. Mao, "Observation of dual-wavelength dissipative solitons in a figure-eight erbium-doped fiber laser," *Opt. Exp.*, vol. 20, no. 19, pp. 20 992–20 997, Sep. 2012.

[8] X. Shan and D. M. Spirit, "Novel method to suppress noise in harmonically mode-locked erbium fibre lasers," *Electron. Lett.*, vol. 29, no. 11, pp. 979–981, May 1993.

[9] C. Wu and N. K. Dutta, "High-repetition-rate optical pulse generation using a rational harmonic mode-locked fiber laser," *IEEE J. Quantum Electron.*, vol. 36, no. 2, pp. 145–150, Feb. 2000.

[10] L. Xu, I. Glesk, D. Rand, V. Bady, and P. R. Prucnal, "Suppression of beating noise of narrow-linewidth erbium-doped fiber ring lasers by use of a semiconductor optical amplifier," *Opt. Lett.*, vol. 28, no. 10, pp. 780–782, May 2003.

[11] M. Yoshida, K. Kasai, and M. Nakazawa, "Mode-hop-free, optical frequency tunable 40-GHz mode-locked fiber laser," *IEEE J. Quantum Electron.*, vol. 43, no. 8, pp. 704–708, Aug. 2007.

[12] D. J. Kuizenga and A. E. Siegman, "FM and AM mode locking of the homogeneous laser—Part I: Theory," *IEEE J. Quantum Electron.*, vol. QE-6, no. 11 pp. 694–708, Nov. 1970.

[13] T. J. Nelson, "A coupled-mode analysis of mode locking in homogeneously broadened lasers," *IEEE J. Quantum Electron.*, vol. QE-8, no. 2 pp. 29–33, Feb. 1972.

[14] H. A. Haus, "A theory of forced mode locking," *IEEE J. Quantum Electron.*, vol. QE-11, no. 7 pp. 323–330, Jul. 1975.

[15] P. Das, W. Kaechele, J. P. Theimer, and A. R. Pirich, "Rational harmonic mode locking fiber laser," *Proc. SPIE*, vol. 3075, pp. 21–32, Mar. 1997.

[16] Y. Jiang *et al.*, "Subharmonic generation in a bandwidth clamped actively mode-locked fiber laser," *IEEE Photon. Technol. Lett.*, vol. 25, no. 23, pp. 2331–2334, Dec. 2013.

[17] N. Onodera, "Supermode beat suppression in harmonically mode-locked erbium-doped fiber ring lasers with composite cavity structure," *Electron. Lett.*, vol. 33, no. 11, pp. 962–963, May 1997.

[18] M.-Y. Jeon *et al.*, "External fibre laser based pulse amplitude equalisation scheme for rational harmonic modelocking in a ring-type fibre laser," *Electron. Lett.*, vol. 34, no. 2, pp. 182–184, Jan. 1998.

[19] Z. Li, C. Lou, K. T. Chan, Y. Li, and Y. Gao, "Theoretical and experiment study of pulse-amplitude-equalization in a rational harmonic mode-locked fiber ring laser," *IEEE J. Quantum Electron.*, vol. 37, no, 1, pp. 33–37, Jan. 2001.

[20] K. K. Gupta, N. Onodera, and M. Hyodo, "Technique to generate equal amplitude, higher-order optical pulses in rational harmonically modelocked fibre ring lasers," *Electron. Lett.*, vol. 37, no. 15, pp. 948–950, Jul. 2001.

[21] S. Yang, K. K. Y. Cheung, X. Xu, Y. Zhou, and K. K. Y. Wong, "Tunable single-longitudinal-mode fiber optical parametric oscillator with saturable-absorber-based auto-tracking filter," in *Proc. OSA/OFC/NFOEC*, Mar. 2010, pp. 1–3.

[22] X. He, D. N. Wang, and C. R. Liao, "Tunable and switchable dual-wavelength single-longitudinal-mode erbium-doped fiber lasers," *J. Lightw. Technol.*, vol. 29, no. 6, pp. 842–849, Mar. 2011.

[23] J. Yang, Y. Jin-Long, W. Yao-Tian, Z. Li-Tai, and Y. En-Ze, "An optical domain combined dual-loop optoelectronic oscillator," *IEEE Photon. Technol. Lett.*, vol. 19, no. 11, pp. 807–809, Jun. 2007.

[24] Y. Jiang *et al.*, "Multifrequency optoelectronic oscillator," *Opt. Eng.*, vol. 53, no. 11, Nov. 2014, Art. ID. 116106.